Can TD–DFT calculations accurately describe the excited states behavior of stacked nucleobases? The cytosine dimer as a test case

ARTICLE *in* JOURNAL OF COMPUTATIONAL CHEMISTRY · APRIL 2008

Impact Factor: 3.59 · DOI: 10.1002/jcc.20853 · Source: PubMed

3 AUTHORS:

Fabrizio Santoro
Italian National Research Council
141 PUBLICATIONS **2,936** CITATIONS
SEE PROFILE

Vincenzo Barone
Scuola Normale Superiore di Pisa
773 PUBLICATIONS **44,695** CITATIONS
SEE PROFILE

Roberto Improta
Italian National Research Council
148 PUBLICATIONS **4,764** CITATIONS
SEE PROFILE

Can TD-DFT Calculations Accurately Describe the Excited States Behavior of Stacked Nucleobases? The Cytosine Dimer as a Test Case

FABRIZIO SANTORO,[1] VINCENZO BARONE,[2] ROBERTO IMPROTA[2,3]

[1] *Istituto per i Processi Chimico-Fisici – CNR, Area della Ricerca del CNR Via Moruzzi, 1 I-56124 Pisa, Italy*

[2] *Dipartimento di Chimica, Università Federico II, Complesso Universitario Monte S. Angelo, Via Cintia, I-80126 Napoli, Italy*

[3] *Istituto di Biostrutture e Bioimmagini – CNR Via Mezzocannone 6, I-80134 Napoli, Italy*

Received 9 July 2007; Accepted 10 September 2007
DOI 10.1002/jcc.20853
Published online 26 October 2007 in Wiley InterScience (www.interscience.wiley.com).

Abstract: By using calculations rooted in the time dependent density functional theory (TD-DFT) we have investigated how the lowest energy excited states of a face-to-face π-stacked cytosine dimer vary with the intermonomer distance (R). The perfomances of different density functionals have been compared, focussing mainly on the lowest energy single excited state of the dimer $(\mathbf{S}_1)_2$. TD-PBE0, TD-LC-ωPBE, and TD-M05-2X provide a picture very similar to that obtained at the CASPT2 level by Merchan et al. (J Chem Phys 2006, 125, 231102), predicting that $(\mathbf{S}_1)_2$ has a minimum for $R \sim 3$ Å, with a binding energy of ~0.5 eV, whereas TD-B3LYP, TD-CAM-B3LYP, and TD-PBE understimate the binding energy. However, independently of the functional employed, no low-energy spurious charge transfer transitions are predicted by TD-DFT calculations, also when a nonsymmetric dimer is investigated, providing encouraging indications for the use of TD-DFT for studying the excited state of π-stacked nucleobases.

 J Comput Chem 29: 957–964, 2008

Key words: excited states; stacking; nucleic acids; time-dependent density functional theory; cytosine

Introduction

Stacking interactions are ubiquitous in chemistry[1] and are the main source of stability for many macromolecular systems of paramount biological and technological interest such as, for example, nucleic acids[2] or porphyrin-like aggregates.[3] The understanding of the excitation, energy, and electron transfer processes in these materials rely on a detailed knowledge of their excited state properties.[4,5] There is thus a largely acknowledged need of reliable and effective computational methods able to describe the excited states of π-stacked aromatic systems. In this respect, methods rooted in time-dependent density functional theory (TD-DFT) are particularly interesting when dealing with large-size systems.[6] However, electronic transitions with significant charge transfer (CT) character are likely present in stacked multimers and the reliability of TD-DFT calculations in treating this kind of transitions has often been questioned.[7] On the other hand, the traditional failures of TD-DFT methods are met in the study of CT transitions between donor–acceptor pairs with vanishing overlap, and this is not the case for the molecular orbitals of two stacked monomers at the typical intermonomer distance of $3 \simeq 4$ Å. As a matter of fact, a recent TD-PBE0 study of a stacked adenine dimer provides results in good agreement with the available experimental indications.[8]

Assessing the reliability of TD-DFT for the excited states of stacked multimers is important, since the limited computational cost of this method could significantly increase the size of the systems that can be treated. Furthermore, the very recent availability of effective TD-DFT geometry optimizations in the condensed phase gives access to the equilibrium geometries and to the properties (dipole moment, polarizability) of the excited states in solution.[9] On these premises a more direct comparison between computations and experiments would be at hand, for systems and processes of significant scientific and technological interest.[10]

Since the interpretation of the experimental results concerning complex systems like stacked aggregates is never straightforward, it would be very important to compare TD-DFT results with those obtained on the same systems by using sophisticate post-Hartree-Fock (HF) calculations. Unfortunately, the number of accurate excited state calculations on medium-size π-stacked dimers is quite

Correspondence to: R. Improta; e-mail: robimp@unina.it

limited.[11,12] However, the very recent publication of a detailed CASPT2 study of π-stacked cytosine dimer provides the interesting possibility of a critical comparison with TD-DFT results.[12] We here thus present a thorough TD-DFT study of a face-to-face π-stacked cytosine dimer. We analyze in detail the performance of six among the most used and/or recently developed density functionals, with the aim of assessing the influence of the employed functionals on the quality of the TD-DFT results. We will examine both a symmetric and a slightly nonsymmetric dimer's coordination, in order to perform a more stringent test of the TD-DFT calculation in a system (the nonsymmetric one) where the occurrence of transitions with partial CT character is not trivially prevented by symmetry.

Computational Details

We have analyzed two different dimer structures, labeled as symmetric, hereafter $(Cyt)_2$, and asymmetric, $(Cyt)_2^{NS}$, performing PBE0/6-31G(d) geometry optimizations of the dimer for a ring–ring distance (R) = 4.0 Å, with a face-to-face orientation (see Fig. 1). In the symmetric case we have imposed a C_S symmetry, and thus the two monomers are constrained to keep the same geometry. In the asymmetric case, we relaxed the symmetry constrain, allowing for the formation of a weak $NH_2\cdots NH_2$ hydrogen bond between the amino groups of the two monomers (see Fig. 1). As a consequence the geometric and electronic structures of the two monomers are no more equivalent. The potential energy surfaces (PES) of the ground and the lowest energy excited electronic states as a function of R have been computed at the TD-DFT/6-31+G(d,p) level, without any further geometry optimization and without any symmetry restrain.

The effect of the basis set superposition error (BSSE) on the ground state energy of the dimer has been taken into account by using the counterpoise method.[13] Checking BSSE effect on the excited states dimerization energies is not straightforward, since the excited states of the dimer can be qualitatively different from those found in the monomer. However, to get an estimate of BSSE on the excited state energies, we have followed an approach similar to that used for the ground state, according to the following equation

$$\mathrm{BSSE}_1(R) = [E_1\mathrm{A} - E_1\mathrm{AB}^*(R)] + [E_1\mathrm{B} - E_1\mathrm{BA}^*(R)] \quad (1)$$

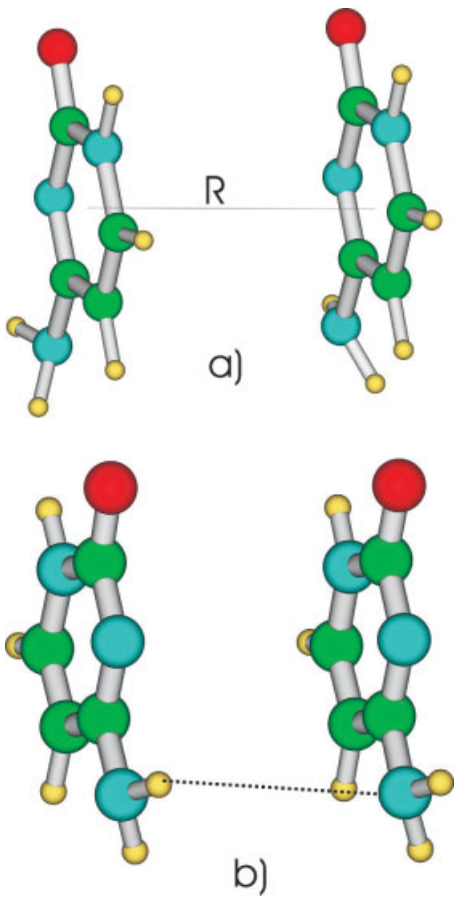

Figure 1. Schematic drawing of the face-to-face π-stacked cytosine dimer. Upper scheme: symmetric dimer; lower scheme: nonsymmetric dimer. [Color figure can be viewed in the online issue, which is available at www.interscience.wiley.com.]

where $E_1\mathrm{A}(E_1\mathrm{B})$ are the energies of the lowest energy excited state of the insulated monomer, while $E_1\mathrm{AB}^*(R)$ and $E_1\mathrm{BA}^*(R)$ are those obtained in the presence of the ghost orbitals of the other monomer (at an intermonomer distance = R). This procedure is expected to be reliable for computing BSSE effects on the energies of the dimer excited states arising from the combination of the S_1 states of the monomers, which are the main targets of our study. Furthermore, since almost all the lowest energy electronic transitions involve the transfer of an electron toward the LUMO of the monomer (vide infra), this procedure is expected to provide a semiquantitative estimate of the BSSE also on the binding energy of the other low energy dimer's excited states. In any case the difference between the BSSE of the ground and of the S_1 excited state is always smaller than 0.03 eV, suggesting that our conclusions should not be qualitatively affected by the method used for estimating the BSSE between the excited states.

We have analyzed some of the most widely used density functionals based on the generalized gradient approximation (GGA) and possibly including some HF exchange (the so-called hybrid functionals). Among the GGA functionals we have chosen the (i) PBE functional,[14] whose exchange and correlation parts, being fully determined by a number of boundary conditions, do not involve any adjustable parameter. Among the hybdrid functionals we have choosen: (ii) the B3LYP, the most widely used hybrid density functional,[15] and (iii) the parameter-free PBE0 hybrid functional,[16] which is the hybrid counterpart of PBE.

We also checked the performance of two recently developed density functionals, specifically designed for a suitable treatment of long-range charge transfer transitions, i.e. (iv) LC-ωPBE [17] and (v) CAM-B3LYP.[18] LC-ωPBE[17] has been built starting from the PBE exhange functional, introducing range separation into the exchange component and replacing the long-range portion of the approximate exchange by its Hartree-Fock counterpart. CAM-B3LYP[18] combines the hybrid qualities of B3LYP and the long-range correction proposed by Hirao and coworkers.[19]

Finally, we performed test calculations using (vi) MO5-2X,[20] which is based on simultaneously optimized exchange and correlation functionals both including kinetic energy density and has shown very good performance in the treatment of dispersion interactions in noncovalent complexes.

In the following we will use PBE0 as a reference functional since, despite the absence of adjustable parameters, it provides accurate excitation energies in several systems,[21] and it has been already successfully applied to the study of nucleobase excited states.[8,22]

All the calculations have been performed by using a development version of Gaussian program.[23]

Results

Before analyzing the results obtained on the dimers, it is important to verify how the different investigated density functionals describe the lowest energy excited states of cytosine monomer. The vertical excitation energies (VEE) computed by using different density functionals, on a geometry optimized at the PBE0/6-31G(d) level, are reported in Table 1. The results delivered by the hybrid PBE0 and B3LYP functionals are very similar to those obtained at the post-HF level.[12,24–28] It is noteworthy that the CASPT2(12,12)/ANO results[12] for the dimer at infinite distance (corresponding to the insulated monomer) are in good quantitative agreement with the experimental results and with previous CASPT2 calculations[24] employing a larger active space on the monomer (CASPT2(12,9)/6-31G(d,p)), at least for the lowest energy $\pi \rightarrow \pi^*$ transition, which is the main object of our analysis.

The $S_0 \rightarrow S_1$ transition is mainly a HOMO$\rightarrow$LUMO excitation, with π/π^* character. $S_0 \rightarrow S_2$ transition can be described as an excitation from the lone pair (LP) localized on the carbonyl group toward the LUMO (n_O/π^*), whereas the $S_0 \rightarrow S_3$ transition corresponds mainly to an excitation from the LP localized on the nitrogen atom of the pyrimidine ring toward the LUMO (n_N/π^*). $S_0 \rightarrow S_1$ is the most intense transition in this energy range, and its VEE is close to the experimental band maximum, lying at $\simeq$4.6 eV (see ref. 28 and references therein). The results provided by the remaining density functionals we investigated are in worse agreement with the CASPT2 indications, especially for what concerns the S_2 and S_3 electronic states. The $S_0 \rightarrow S_1$ transition always corresponds to the bright π/π^* excitation (with the exception of the TD-PBE results), although the computed VEE is somewhat overestimated with respect to the experimental results.

TD-PBE0 test calculations indicate that the 6-31+G(d,p) results are not significantly different from those obtained by using the more extended 6-311+G(2d,2p) basis set. Most of the calculations on cytosine dimers have thus been performed at the 6-31+G(d,p) level.

Table 1. Computed VEE in the Gas Phase for Cytosine by Using Different Density Functionals and the 6-31+G(d) Basis Set on a Geometry Optimized at the PBE0/6-31G(d) Level.

	Energy (osc. str.)	Orbitals	Description
CASPT2/6-31G(d,p)[a]			
S1	4.50 (0.065)	H→L	π/π^*
S2	4.88 (0.001)		n_O/π^*
S3	5.23 (0.003)		n_N/π^*
PBE0			
S1	4.79 (0.049)	H→L	π/π^*
S2	4.97 (0.002)	H-1→L	n_O/π^*
S3	5.38 (0.001)	H-3→L	n_N/π^*
PBE			
S1	3.85 (0.000)	H-1→L	n_O/π^*
S2	4.25 (0.020)	H→L	π/π^*
S3	4.53 (0.002)	H-3→L	n_N/π^*
LC-ωPBE			
S1	5.03 (0.075)	H→L	π/π^*
S2	5.22 (0.002)	mixed→L	n/π^*
S3	5.89 (0.001)	mixed→L+3	n/π^*
B3LYP			
S1	4.68 (0.043)	H→L	π/π^*
S2	4.80 (0.001)	H-1→L	n_O/π^*
S3	5.16 (0.001)	H-3→L	n_N/π^*
CAM-B3LYP			
S1	4.98 (0.070)	H→L	π/π^*
S2	5.29 (0.003)	mixed→L	n/π^*
S3	5.78 (0.004)	H→L+1	π/π^*
M05-2X			
S1	5.12 (0.082)	H→L	π/π^*
S2	5.35 (0.002)	mixed→L	n/π^*
S3	5.87 (0.000)	mixed→L+2	n/π^*

Oscillator strengths are given in parentheses.
PBE0/6-31G(d) results: S1 4.86 (0.04); S2 4.97 (0.001); S3 5.38 (0.001); PBE0/6-311+G(2d,2p) results: S1 4.75 (0.05); S2 4.95 (0.002); S3 5.36 (0.00); experiments: $\simeq$4.6 eV; see values collected in ref. 28.
[a]See ref. 24.

Symmetric Dimer

We start our analysis from the TD-PBE0 results. In Figure 2 are reported the potential energy curves of the ground and the 10 lowest energy excited electronic states varying the intermonomer distance (R) between 5.6 and 2.6 Å.

Even if the present study is focussed on the calculation of the excited states, it is noteworthy that according PBE0 calculations no energy minimum along R is present for the ground state, and its energy steeply increases for $R \leq 3.2$ Å. This picture is very similar to that provided by CASPT2 calculations,[12] which also predicts the dimer is not bound in the ground state. However, the computed CASPT2 PES is less repulsive than the PBE0 counterpart (by $\approx$0.3 eV at $R = 3$ Å). This result is not suprising, since PBE0, and more in general "standard" DFT funtionals are known to underestimate the binding energy of stacked aromatic dimers.[17,20,29–33] On the other hand, as we shall see later, the results of M05-2X and LC-ωPBE calculations are extremely similar to those of the CASPT2 level also for what concerns the ground state PES.

All the adiabatic excited states, except the lowest energy one, change their nature along the path. Basically, for $R \geq 3.1$ Å, the lowest energy excited states involve the combinations of the frontier orbitals of the monomers, i.e. those involved in the π/π^*, n_O/π^*, n_N/π^* transitions of the monomer. For $R \leq 3$ Å, electronic

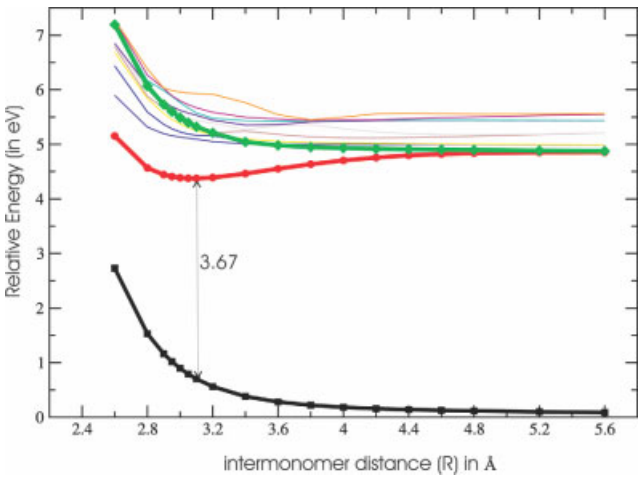

Figure 2. Potential energy surface of the ground and the 10 lowest adiabatic excited states of $(Cyt)_2$ as a function of the intermonomer distance (R). The bold curves correspond to diabatic excited states $(\mathbf{S}_1)_2$ (circle) and $(\mathbf{S}_2)_2$ (diamonds). [Color figure can be viewed in the online issue, which is available at www.interscience.wiley.com.]

excitations to Rydberg orbitals contribute to some of the excited electronic states [for example, $(S_5)_2$ and $(S_6)_2$].

In the following we shall focus essentially on the electronic states that are related to the monomer's π/π^* lowest energy excited state [labeled $(\mathbf{S}_1)_2$ and $(\mathbf{S}_2)_2$, respectively, and corresponding to the bold curves (circles and diamonds) in Fig. 2], since in the reference CASPT2 study of $(Cyt)_2$ only the π orbitals of cytosine are included in the active space.[12] To this end, it is necessary to analyze in some detail the shape of the four frontier orbitals of $(Cyt)_2$, for $R \geq 3.0$ Å, arising from the symmetric and antisymmetric combinations of the two HOMOs and the two LUMOs of the monomers (see Fig. 3). Even if the energy ordering of the $(Cyt)_2$ molecular orbitals changes along the path, $(HOMO)_2$ always corresponds to the antisymmetric combination (with antibonding character) of monomer HOMOs, whereas $(LUMO)_2$ is the symmetric combination of the monomers' LUMO and is stabilized by their bonding interaction. On the contrary, the symmetric combinations of the HOMOs and the antisymmetric combination of the LUMOs are stabilized and destabilized, respectively, with respect to the HOMO and the LUMO of the monomer. Four different electronic transitions can be obviously associated to the above molecular obitals. On the ground of the above considerations (see also Fig. 3), we can expect that one of the four resulting electronic transitions [corresponding to the $(HOMO)_2 \rightarrow (LUMO)_2$ excitation] is remarkably stabilized with respect to the monomer, and that the amount of the stabilization increases when R decreases. As a matter of fact, this state $[(\mathbf{S}_1)_2]$ always corresponds to the lowest energy adiabatic state and exhibits a rather deep minimum for $R = 3.1$ Å. The binding energy of $(\mathbf{S}_1)_2$ is 0.48 eV, and the emission energy is 3.67 eV, i.e. 1.12 eV smaller than for the insulated cytosine. This picture is extremely similar to that obtained at the CASPT2(12,12)/ANO level, providing a minimum for $(\mathbf{S}_1)_2$ for $R = 3.076$ Å, with a binding energy of 0.58 eV and an emission energy of 3.40 eV, i.e 1.01 smaller than for the insulated monomer.[12]

Before proceeding to our analysis of $(\mathbf{S}_1)_2$, it can be useful to examine in some detail the behavior of the other excited states. For $(\mathbf{S}_2)_2$, the discrepancy between TD-PBE0 and CASPT2 results is larger than that found for $(\mathbf{S}_1)_2$, even if the picture provided by the two methods is not dramatically different. Indeed, TD-PBE0 calculations predict that the energy of the $(\mathbf{S}_2)_2$ is almost constant up to $R \simeq 4$ Å, and then it starts increasing rather steeply. On the other hand, CASPT2 predicts the existence of a very shallow minimum for $R = 3.4$ Å, with a small binding energy (0.25 eV). Finally, it is worth of noting that, besides $(\mathbf{S}_1)_2$, there are two additional low energy excited states that exhibit a minimum along R. They are related, respectively, to the n_O/π^* and n_N/π^* transitions of the monomer. This result is not suprising, because both the above excited states involve the transfer of an electron to the $(LUMO)_2$, whose energy decreases along R. However, the binding energy of these two latter minima is lower than that of $(\mathbf{S}_1)_2$, since the energy of the n_O and n_N molecular orbitals does not exhibit the marked dependence on R shown by the π $(HOMO)_2$ orbital.

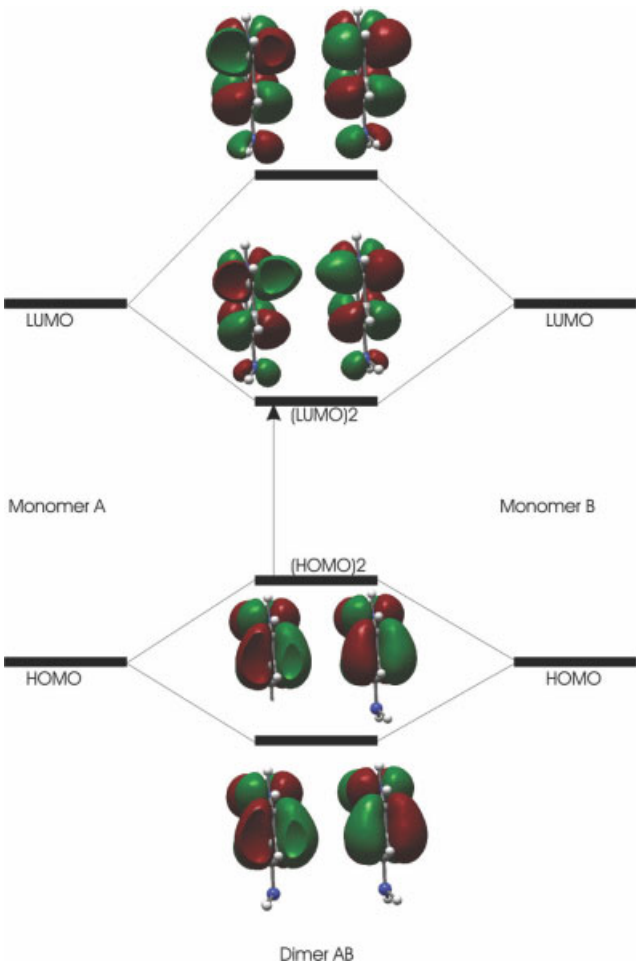

Figure 3. Schematic drawing of the frontier orbitals of $(Cyt)_2$. [Color figure can be viewed in the online issue, which is available at www.interscience.wiley.com.]

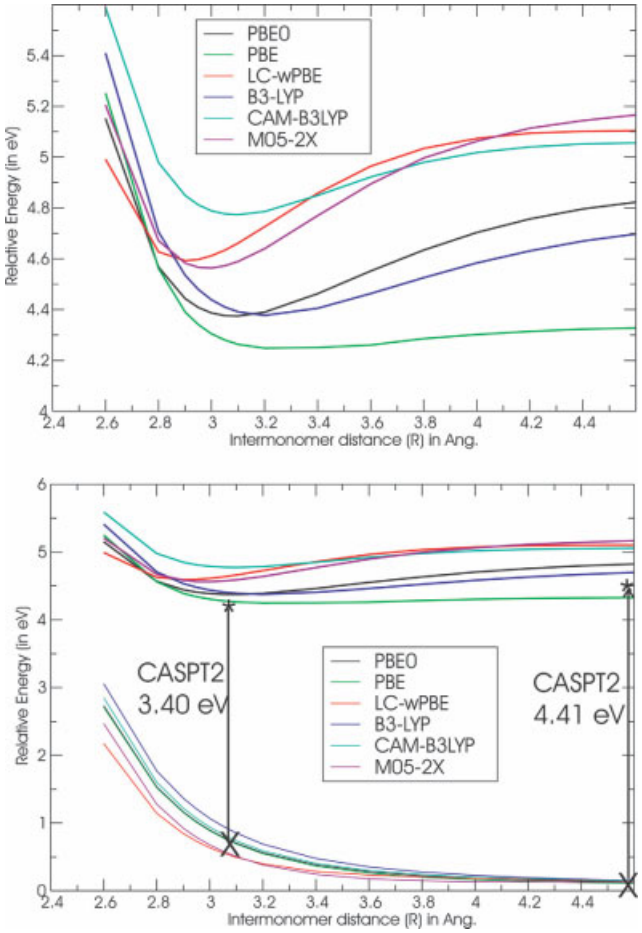

Figure 4. Potential energy surface of the ground and $(S_1)_2$ excited state of $(Cyt)_2$ as a function of the intermonomer distance (R), computed employing different functionals (lower figure). Closer view on the excited state PES (upper figure). DFT and TD-DFT 6-31+G(d,p) calculations. CASPT2 results[12] are also shown for comparison.

Comparison Between Different Density Functionals

The PES of $(S_0)_2$ (the ground state of the dimer) and $(S_1)_2$ computed at the TD-DFT level by employing different density functionals are reported in Figure 4 (see also Table 2). TD-DFT calculations, independently of the density functional employed, predict the existence of a minimum along R for $(S_1)_2$ (namely, $(S_1)_2$-**min**). However, from a quantitative point of view, the different functionals provide a rather different description of $(S_1)_2$-**min**. Indeed, three functionals, namely B3LYP, CAM-B3LYP, and, especially, PBE significantly underestimate the binding energy of $(S_1)_2$-**min** with respect to the CASPT2 results. B3LYP and PBE also predict that the minimum is found for $R = 3.2$ Å, a value ≈0.12 Å larger than the CASPT2 result. Finally, PBE significantly underestimates the red-shift of the S_1-S_0 energy gap at $(S_1)_2$-**min** with respect to the monomer.

LC-ωPBE and M05-2X exhibit in a sense the opposite behavior with respect to the three functionals examined above. Indeed the relative emission energy is slightly larger and R at the minimum slightly shorter than the CASPT2 prediction. However, it is important to highlight that these functionals, together with PBE0, provide a description of the $(S_1)_2$ PES very close to that provided by CASPT2 calculations.

Nonsymmetric Dimer

As shown in Figure 5, TD/PBE0 calculations indicate that in the nonsymmetric dimer, as expected, the nonequivalence of the two monomers causes a small asymmetrization of the frontier orbitals. $(HOMO)_2$ receives a larger contribution from one of the monomers while the opposite occurs for $(LUMO)_2$. As a consequence the $(S_1)_2$ electronic state exhibits a partial CT character, $0.15 \simeq 0.2$ a.u (depending on R) according to TD-PBE0/6-31+G(d,p) calculations. Notwithstanding the partial CT character of $(S_1)_2$, the PES along R is very similar to that predicted for the symmetric case, and, specifically no unphysical stabilization of $(S_1)_2$ is predicted (see Figure 6). The relative performance of the different functionals examined are also very similar to that found for $(Cyt)_2$. Indeed LC-ωPBE results are very similar to those provided by PBE0. B3LYP and CAM-B3LYP underestimate the binding energy of the minimum and PBE provides an extremely shallow and weak minimum.

Concluding Remarks

The present study provides encouraging indications about the reliability of TD-DFT calculations, when based on a suitable functional, for the treatment of the excited states in π-stacked nucleobases. As a matter of fact, the description of the $(Cyt)_2$ lowest energy excited state for different intermonomer distances obtained by using TD-PBE0, TD-LC-ωPBE, and TD-M052X methods is extremely similar to that provided by sophisticate and expensive CASPT2 calculations.

Table 2. Interatomic Distance of the Minimum (R_{min} in Å), Binding, Emission, and Relative Emission (with Respect to the Monomer) Energies (in eV) of the $(S_1)_2$ State According to Different Computational Methods.

Method	R_{min}	E binding	E emission	Relative emission
Symmetric dimer				
CASPT2	3.08	0.58	3.40	1.01
TD-PBE0	3.10	0.48	3.67	1.12
TD-PBE	3.2	0.10	3.70	0.55
TD-LC-ωPBE	2.9	0.52	3.75	1.28
TD-B3LYP	3.2	0.34	3.69	0.99
TD-CAM-B3LYP	3.1	0.31	4.04	0.94
TD-M05-2X	3.0	0.61	3.89	1.23
Nonsymmetric dimer				
TD-PBE0	3.14	0.52	3.66	1.11
TD-PBE	3.64	0.10	3.92	0.33
TD-LC-ωPBE	2.94	0.55	3.77	1.30
TD-B3LYP	3.24	0.37	3.67	0.97
TD-CAM-B3LYP	3.14	0.34	4.04	0.94

The 6-31+G(d,p) basis set has been employed in the TD-DFT calculations.

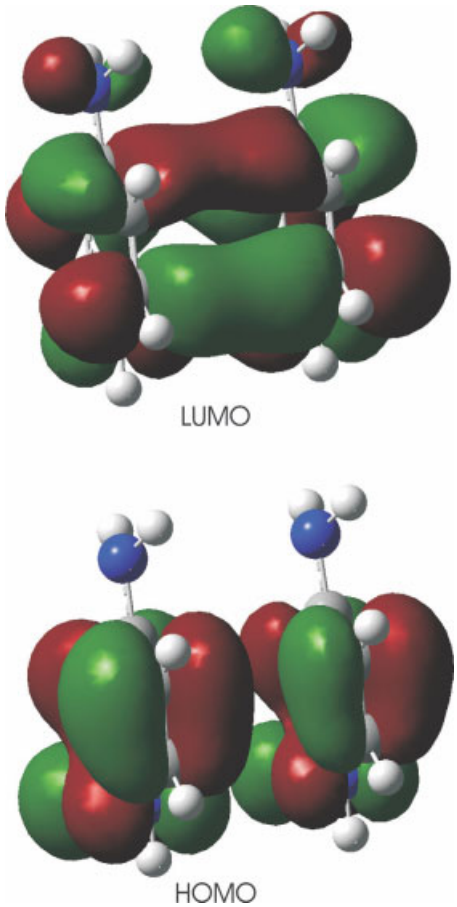

Figure 5. Schematic drawing of the frontier orbitals of $(Cyt)_2^{NS}$. [Color figure can be viewed in the online issue, which is available at www.interscience.wiley.com.]

This result can be explained considering that the failures of TD-DFT calculations usually occur for long-range CT between two partners whose molecular orbitals have a vanishing overlap.[7] This is obviously not the case of stacked aromatic molecules with a interring distance of ~3.5 Å, whose molecular orbitals are significantly mixed, and which can thus be considered as a supermolecule. Actually, the existence of a minimum along R for $(\mathbf{S}_1)_2$ [deriving from the $(HOMO)_2 \rightarrow (LUMO)_2$ transition] is ruled by the strong dependence of the energy of the frontier molecular orbitals on the intermonomer distance. For example, the energy of $(HOMO)_2$ and $(LUMO)_2$ changes, in opposite directions, by more than 0.5 eV along R. We believe that this is the most significant effect modulating the behavior of $(\mathbf{S}_1)_2$, and, indeed, all the density functionals indicate that this state has a minimum along R.

The choice of the functional affects instead the features of the minimum. The binding energy predicted by B3LYP and CAM-B3LYP is too low when compared to CASPT2 results. This result is probably due to the overestimation of the van der Waals repulsive interactions usually associated to the Becke exchange functional. As a matter of fact, the ground state PES exhibiting the most significant destabilization upon decrease of R is that computed at the B3LYP and CAM-B3LYP level. This result is not surprising taking into account that a correct treatment of nonbonding interactions critically depends on the behavior of the functional in the low-density/high-gradient regions,[30–35] such as that involved in a stacked interaction. The Becke exchange functional, not obeying the Levy condition[36] nor the Lieb-Oxford bound,[37] exhibits an incorrect asympototic limit and a quite poor behavior in that region. CAM-B3LYP is based on the same exchange functional and indeed it also underestimated the binding energy of $(\mathbf{S}_1)_2$.

On the balance, the poorest performance is that exhibited by the PBE calculations, indicating the importance of inclusion of a part of HF exchange in the exchange functional for a correct description of excited states and intermolecular interactions. It is also noteworthy that TD-PBE is the only method predicting that the lowest energy electronic transition in the monomer does not correspond to the HOMO→LUMO (π/π^*) excitation.

When considering the results concerning both the monomer and the dimers, TD-PBE0 probably provides the closest results to

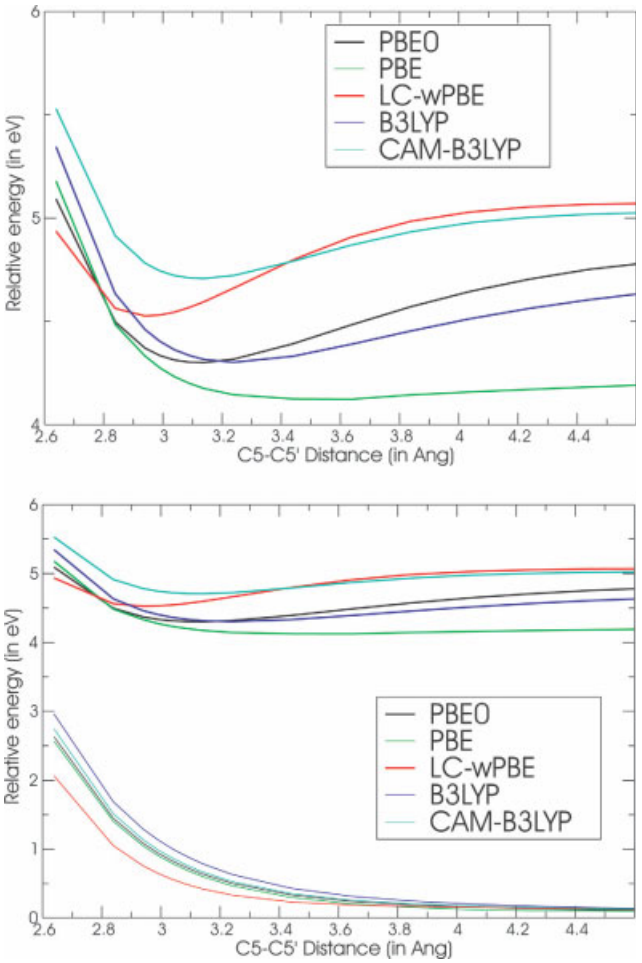

Figure 6. Potential energy surface of the ground and $(\mathbf{S}_1)_2$ excited state of $(Cyt)_2^{NS}$ as a function of the intermonomer distance (R), computed employing different functionals (lower figure). Closer view on the excited state PES (upper figure). DFT and TD-DFT 6-31+G(d,p) calculations.

CASPT2 ones. On the other hand, LC-ωPBE and M05-2X, which are purposely tailored for a correct description of long range effects, allow for a more accurate treatment of the van der Waals interactions in the dimer. As a consequence, the curve associated to the ground state is less repulsive than that predicted by PBE0 (and closer to the CASPT2 one) and the binding energy of $(S_1)_2$-**min** is larger.

It is remarkable that in the nonsymmetric dimer, although the $(\mathbf{S}_1)_2$ state acquires a partial CT transfer, its energy does not receive any dramatic overstabilization, and that there is no sign of other spurious low-lying CT state. Not only the binding energy of $(\mathbf{S}_1)_2$ does not significantly change, but the shape of the curve along R is similar to that obtained for the $(\mathrm{Cyt})_2$. This result provides an additional indication that the "good" performance of some TD-DFT methods is not an artefact due to the equivalence of the monomers in the symmetric dimer.

Although any single system has to be examined in detail, the results hereby reported, together with our previous study on stacked adenine multimers, provide encouraging indications about the possibility of getting a reliable description of the excited state behavior of stacked aromatic macromolecular aggregates by using a suitable TD-DFT method. When the number of monomers increases it is obviously necessary to check that artificially low-lying long-range CT transitions between "distant" monomers do not bias the accuracy of the computational description. In this respect it is noteworthy that some of the recently developed functionals (LC-ωPBE, M05-2X, CAM-B3LYP) have shown to provide reliable results for this kind of transitions as well.[38] On the balance, TD-DFT is confirmed to be a promising tool for studying complex/large systems, not only for the size of the systems that can be treated but also because it gives the possibility of describing different excited states on the same footing and with the same degree of accuracy, limiting the number of *a priori* choices. Inspection of Figure 2 clearly indicates that several excited states (not only those with π/π^* character) could in principle modulate the excited state properties of cytosine dimer. These electronic states could be strongly vibronically coupled and thus there are many processes, for example, those involved in ultra-fast time-resolved experiments, that can be understood only considering, contemporarily, several interacting electronic states. On one hand, this feature often poses severe limitations on the usefulness of any approach based only on the static description of a limited number of noninteracting adiabatic electronic states. On the other hand, it is clear that a complete and unbiased description of many excited states for a wide range of structures is very important for any theoretical study.

References

1. (a) Hobza, P.; Selzle, H. L.; Schlag, E. W. Chem Rev 1994, 94, 1767; (b) Meyer E. A.; Castellano R. K.; Diederich, F. Angew Chem Int Ed 2003, 42, 1210; (c) McGaughey, G. B.; Gagne, M.; Rappe, A. K. J Biol Chem 1998, 273, 15458; (d) Muller-Dethlefs, K.; Hobza, P. Chem Rev 2000, 100, 143; (e) Kim, K. S.; Tarakeshwar, P.; Lee, J. Y. Chem Rev 2000, 100, 4145.
2. (a) Hobza, P.; Sponer, J. Chem Rev 1999, 99, 3247; (b) Yakovchuk, P.; Protozanova, E.; Frank-Kamenetskii, M. D. Nucleic Acids Res 2006, 34, 564; (c) Luo, R.; Gilson, H. S.; Potter, M. J.; Gilson, M. K. Biophys J 2001, 80, 140.
3. Kobayashi, T., Ed. J-Aggregates; World Scientific: Singapore, 1996.
4. (a) Crespo-Hernandez, C. E.; Cohen, B.; Kohler, B. Nature 2005, 436, 1141; (b) Crespo-Hernandez, C. E.; Cohen, B.; Kohler, B. Chem Rev 2004, 104, 1977.
5. (a) Tretiak, S.; Mukamel, S. Chem Rev 2002, 102, 3171; (b) Akins D. L.; Ozcelik, S.; Zhu, H. R.; Guo, C. J Phys Chem 1996, 100, 14390; (c) Ohno, O.; Kaizu, Y.; Kobayashi, H. J Chem Phys 1993, 99, 4128; (d) Chen, P.; Tomov, I. V.; Dvovnikov, A. S.; Nakashima, M.; Roach, J. F.; Alabram, D. M.; Rentzepis, P. M. J Phys Chem 1996, 100, 17507; (e) Karotki, A.; Drobizhev, M.; Kruk, M.; Spangler, C.; Nickel, E.; Mamardashvili, N.; Rebane, A. J Opt Soc Am B 2003, 20, 321.
6. Casida, M. E.; Chong, D. P., Eds. Recent Advances in Density Functional Methods, Vol. 1; World Scientific; Singapore, 1995.
7. (a) Dreuw, A.; Head-Gordon, M. Chem Rev 2005, 105, 4009; (b) Wanko, M.; Garavelli, M.; Bernardi, F.; Niehaus, T. A.; Frauenheim, T.; Elstner, M. J Chem Phys 2004, 120, 1674; (c) Dreuw, A.; Weisman, J. L.; Head-Gordon, M. J Chem Phys 2003, 119, 2943; (d) Dreuw, A.; Head-Gordon, M. J Am Chem Soc 2004, 126, 4007; (e) Tozer, D. J.; Amos, R. D.; Handy, N. C.; Roos, B. O.; Serrano-Andres, L. Mol Phys 1999, 97, 859.
8. Santoro, F.; Barone, V.; Improta, R. Proc Nat Acad Sci USA 2007, 104, 9931.
9. Scalmani, G.; Frisch, M. J.; Mennucci, B.; Tomasi, J.; Cammi, R.; Barone, V. J Chem Phys 2006, 124, 094107.
10. (a) Improta, R.; Barone, V.; Santoro, F. Angew Chem Int Ed 2007, 46, 405; (b) Santoro, F.; Improta, R.; Lami, A.; Bloino, J.; Barone V. J Chem Phys 2007, 126, 084509; J Chem Phys 2007, 126, 169903 (erratum); (c) Santoro, F.; Lami, A.; Improta, R.; Barone, V. J Chem Phys 2007, 126, 184102.
11. Rocha-Rinza, T.; De Vico, L.; Veryazov, V.; Roos, B. O. Chem Phys Lett 2006, 426, 268.
12. Olaso-Gonzalez, G.; Roca-Sanjuan, D.; Serrano-Andrés, L.; Merchán M. J Chem Phys 2006, 125, 231102.
13. Boys, S. F.; Bernardi, F. Mol Phys 1970, 19, 553.
14. Perdew, J. P.; Burke, K.; Ernzerhof, M. Phys Rev Lett 1996, 77, 3865.
15. Becke, A. D. J Chem Phys 1993, 98, 5648.
16. (a) Adamo, C.; Barone, V. J Chem Phys 1999, 110, 6158; (b) Enzerhof, M.; Scuseria, G. E. J Chem Phys 1999, 110, 5029.
17. Vydrov, O. A.; Scuseria, G. E. J Chem Phys 2006, 125, 234109.
18. Yanai, T.; Tew, D. P.; Handy, N. C. Chem Phys Lett 2004, 393, 51.
19. Tawada, Y.; Tsuneda, T.; Yanagisawa, S.; Yanai, T.; Hirao, K. J Chem Phys 2004, 120, 8425.
20. Zhao, Y.; Schultz, N. E.; Truhlar, D. G. J Chem Theory Comput 2006, 2, 364.
21. Adamo, C.; Scuseria, G. E.; Barone, V. J Chem Phys 2000, 111, 2889.
22. (a) Gustavsson, T.; Banyasz, A.; Lazzarotto, E.; Markovitsi, D.; Scalmani, G.; Frisch, M. J.; Barone, V.; Improta, R. J Am Chem Soc 2006, 128, 607; (b) Santoro, F.; Barone, V.; Gustavsson, T.; Improta, R. J Am Chem Soc 2006, 128, 16312; (c) Improta, R.; Barone, V. J Am Chem Soc 2004, 126, 14320.
23. Frisch, M. J.; Trucks, G. W.; Schlegel, H. B.; Scuseria, G. E.; Robb, M. A.; Cheeseman, J. R.; Montgomery, J. A.; Vreven, T. Jr.; Scalmani, G.; Kudin, K. N.; Iyengar, S. S.; Tomasi, J.; Barone, V.; Mennucci, B.; Cossi, M.; Rega, N.; Petersson, G. A.; Nakatsuji, H.; Hada, M.; Ehara, M.; Toyota, K.; Fukuda, R.; Hasegawa, J.; Ishida, M.; Nakajima, T.; Honda, Y.; Kitao, O.; Nakai, H.; Li, X.; Hratchian, H. P.; Peralta, J. E.; Izmaylov, A. F.; Heyd, J. J.; Brothers, E.; Staroverov, V.; Zheng, G.; Kobayashi, R.; Normand, J.; Burant, J. C.; Millam, J. M.; Klene, M.; Knox, J. E.; Cross, J. B.; Bakken, V.; Adamo, C.; Jaramillo, J.; Gomperts, R.; Stratmann, R. E.; Yazyev, O.; Austin, A. J.; Cammi, R.; Pomelli, C.; Ochterski, J. W.; Ayala, P. Y.; Morokuma, K.; Voth, G. A.; Salvador, P.; Dannenberg, J. J.; Zakrzewski, V. G.; Dapprich, S.; Daniels, A. D.; Strain, M. C.;

Farkas, O.; Malick, D. K.; Rabuck, A. D.; Raghavachari, K.; Foresman, J. B.; Ortiz, J. V.; Cui, Q.; Baboul, A. G.; Clifford, S.; Cioslowski, J.; Stefanov, B. B.; Liu, G.; Liashenko, A.; Piskorz, P.; Komaromi, I.; Martin, R. L.; Fox, D. J.; Keith, T.; Al-Laham, M. A.; Peng, C. Y.; Nanayakkara, A.; Challacombe, M.; Chen, W.; Wong, M. W.; Pople, J. A.; Gaussian Development Version, Revision F.01, Gaussian, Inc., Wallingford CT, 2006.

24. Merchan, M.; Serrano-Andrés, L. J Am Chem Soc 2003, 125, 8108.
25. Kistler, K. A. ; Matsika, S. J Phys Chem A 2007, 111, 2650.
26. Ismail, N.; Blancafort, L.; Olivucci, M.; Kohler, B.; Robb, M. J Am Chem Soc 2002, 124, 6818.
27. (a) Sobolewski, A. L.; Domcke, W. Phys Chem Chem Phys 2004, 6, 2763; (b) Tomic, K.; Jörg, T.; Marian, C. M. J Phys Chem A 2005, 109, 8410.
28. Fuelscher, M. P.; Roos, B. O. J Am Chem Soc 1995, 117, 2089.
29. Improta, R.; Barone, V. J Comput Chem 2004, 25, 1333.
30. Adamo, C.; Barone, V. J Chem Phys 1998, 108, 664.
31. (a) Kamiya, M.; Tsuneda,T.; Hirao, K. J Chem Phys 2002, 117, 6010; (b) Tsuneda, T.; Suzumura, T.; Hirao, K. J Chem Phys 1999, 110, 10664.
32. Wu, X.; Vargas, M. C.; Nayak, S.; Lotrich, V.; Scoles, G. J Chem Phys 2001, 115, 8748.
33. Wesolowski, T. A.; Parisel, O.; Ellinger, Y.; Weber, J. J Phys Chem A 1997, 101, 7818.
34. Zhang, Y.; Pan, W.; Yang, W. J Chem Phys 1997, 107, 7921.
35. Lacks, D. J.; Gordon, R. G. Phys Rev A 1993, 47, 4681.
36. Levy, M.; Perdew, J. P. Phys Rev B 1993, 48, 11638.
37. Lieb, E. H.; Oxford, S. Int J Quantum Chem 1981, 19, 427.
38. (a) Cai, Z. L.; Crossley, M. J.; Reimers, J. R.; Kobayashi, R.; Amos, R. D. J Phys Chem B 2006, 110, 15624; (b) Kobayashi, R.; Amos, R. D. Chem Phys Lett 2006, 420, 106; (c) Peach, M. J. G.; Helgaker, T.; Salek, P.; Keal, T. W.; Lutnaes, O. B.; Tozer, D. J.; Handy, N. C. Phys Chem Chem Phys 2006, 8, 558; (d) Zhao, Y.; Schultz, N. E.; Truhlar, D. G. J Chem Theor Comput 2006, 2, 364; (e) Zheng, J. J.; Zhao, Y.; Truhlar, D. G. J Phys Chem A 2007, 111, 4632.